P150275.PDF [Page: 3 of 14]

THE USE OF ELECTROCHEMICAL IMPEDANCE SPECTROSCOPY TO PREDICT THE CORROSION OF ALUMINUM-LITHIUM ALLOYS IN MARINE ENVIRONMENTS

D. R. Lenard and J. G. Moores
Defence Research Establishment Pacific
FMO Victoria, B.C., Canada V0S 1B0
P. R. Roberge and E. Halliop
Royal Military College of Canada
Kingston, ON, Canada K7L 2W3

SUMMARY

In order to acquire some experience with the behaviour of aluminum-lithium alloys in the marine environment, the Defence Research Establishment Pacific compared panels made from Aluminum Alloy (AA) 2090 and 8090 sheet with the conventional alloys AA 7075 and 2024, respectively, in several tests involving long term exposure to sea water fog and full or partial immersion in sea water. The results of these tests were then compared with the results of a new technique, developed by the Royal Military College of Canada for the analysis of electrochemical impedance measurements, that was performed on these alloys in simulated sea water. The long term exposure tests indicated that corrosion problems could occur with aluminum-lithium alloys in the marine environment. The 8090 alloy was found to suffer from severe localized attack, including intergranular cracking, along edges that were immersed in sea water. The 2090 alloy, however, appeared to offer some advantages over its 7075-T6 counterpart, as it was more resistant to corrosion at its edges, even though it suffered as much or more corrosion on the rolled surfaces. On some 2090 panels, the corrosion resistance of the edges was found to be enhanced by cold work associated with shearing. Polarization resistance measurements were generally consistent with the results of the long term exposure tests, although they predicted corrosion rates for the rolled surfaces of the 8090 and 7075 alloys that were apparently too high. The angle of depression of the Nyquist plots appeared to correlate with the number of corrosion sites within a given area and was in good agreement with visual observations of the long term exposure panels.

INTRODUCTION

Aircraft designers, manufacturers and operators are continually seeking new materials for aircraft structures that have higher strength-to-weight ratios in order to achieve significant weight reductions. A lighter airframe can result in lower fuel consumption, longer range, higher acceleration and/or heavier payloads. This search has led to heightened interest in the development and use of aluminum-lithium alloys. These alloys offer the promise of lower density, higher elastic modulus, higher strength and improved thermal stability when compared to conventional aluminum alloys[1,2].

Historically, improvements in mechanical properties with new alloys have often resulted in increases in susceptibility to corrosion that were not adequately studied prior to the specification of these alloys in aircraft structures. For example, aircraft designers were quick to specify the T6 temper of AA 7075 because of its high modulus and strength. It was subsequently discovered to be highly susceptible to stress corrosion and exfoliation in marine environments at great cost to aircraft operators[3]. As a result of this history and because elemental lithium is extremely reactive, there has been considerable interest in the corrosion susceptibility of aluminum-lithium alloys. A variety of accelerated corrosion tests[4] and standard electrochemical techniques[5,6] have been used to study the corrosion behaviour of Al-Li. No consistent picture of the corrosion resistance of these alloys has yet emerged. Although there is general agreement that localized corrosion can occur in these alloys, there are differences of opinion about the relative susceptibilities between different Al-Li alloys and with respect to conventional alloys[7-10].

The Canadian Department of National Defence had been planning to acquire a new helicopter to replace its existing Sea King and Labrador fleets. The manufacturer of this helicopter favoured the extensive use of Al-Li sheet, extruded profiles and forgings. In order to acquire some first hand experience with the behaviour of these alloys in the marine environment, the Defence Research Establishment Pacific (DREP) subjected panels made from AA 2090 and 8090 sheet, along with 2024 and 7075 sheet, to several tests involving exposure to sea water fog and full or part immersion in sea water. The results of these tests were then compared with the results of a new technique developed and performed by the Royal Military College of Canada for the analysis of electrochemical impedance measurements on these alloys in simulated sea water.

ELECTROCHEMICAL IMPEDANCE SPECTROSCOPY

In recent years, electrochemical impedance spectroscopy (EIS) has found increasing use in the investigation of the mechanisms and rates of corroding systems. The nondestructive nature of the test, the short time needed to attain reproducible results and the need for electrochemical monitoring of corrosion processes in situ have all contributed to the growing acceptance of this method.

EIS data can be obtained by applying a small sinusoidal

Paper presented at the 79th Meeting of the AGARD Structures and Materials Panel on "Corrosion Detection and Management of Advanced Airframe Materials" held in Seville, Spain, 5-6 October 1994.

P150275.PDF [Page: 4 of 14]

current signal to a specimen and measuring the amplitude and phase shift of the resulting voltage. For many corroding interfaces, EIS measurements taken over a wide range of frequencies show a circular arc in the complex impedance plane when the real and imaginary components are plotted against each other in a Nyquist plot[11,12]. By examining the impedance at appropriate frequencies, accurate values of the polarization resistance can be determined. Using the Stern-Geary equation, corrosion rates can be obtained as an inverse function of the polarization resistance[13]. In many systems of practical interest, analysis of EIS data is complicated by the fact that the Nyquist plots exhibit depression below the real axis, and by low corrosion rates which make it difficult to obtain reproducible results at all frequencies. Roberge and co-workers[14-16] have recently developed statistical and geometric analysis techniques that have overcome these difficulties. Their procedure yields reliable values for both the polarization resistance and the angle of depression. In a recent study of mild steel specimens in inhibited sodium chloride solutions, they were able to obtain overall corrosion rates from the polarization resistance and to show a correlation between the angle of depression and the extent of localized corrosion (pitting)[17].

EXPERIMENTAL PROCEDURE

The 76 x 76 mm panels used in the exposure tests were sheared from sheets made of Aluminum Alloys 2024-T3, 2090-T8, 7075-T6 and 8090-T851. Specimens made from AA 6061-T6, an alloy commonly used in marine applications, were included in the exposure tests and appear in some photographs but were not part of the comparison with electrochemical experiments. The nominal compositions of these alloys are shown in Table 1. Both surfaces of each panel were sanded with 120 grit silicon carbide abrasive paper and each panel was then fitted with two ceramic multiple-crevice washers (designed according to ASTM G78) that were held in place with a #12 stainless steel nut and bolt assembly that passed through a 6.3 mm central hole. Each bolt was fitted through plastic tubing to prevent contact with the aluminum panel. Each washer provided twelve separate sites for initiation of crevice corrosion. Each panel was suspended by way of a plastic-coated wire that was passed through a 3 mm hole that had been drilled in one corner of the specimen.

One set of specimens was exposed to a sea water fog at 35°C for four months in an Atlas SF850 Corrosive Fog Exposure System. The exposure was conducted according to ASTM B117 with the exception that natural sea water was used to generate the fog instead of the standard sodium chloride solution.

The remaining specimens were suspended in sea water that was drawn from the Strait of Juan de Fuca and directed through a tank measuring 16 X 62 x 177 cm. The sea water flowed past any specimen immersed in it at a rate of 1 cm/sec and was then returned to the Strait 40 m from the intake. The water temperature in this location is within the range 7-11°C throughout the year. One set was suspended in a single row perpendicular to the direction of flow so that one half of the specimen was under water. A second set was suspended in a single row 1 m downstream from the first so that the entire specimen was immersed.

All specimens were removed after an exposure time of four months. After the specimens were dismantled the aluminum panels were cleaned by immersion in concentrated nitric acid. They were then rinsed with distilled water and allowed to dry after a final rinse with ethanol. Sections were cut from the panels and set in epoxy according to standard metallographic techniques in an effort to determine the depth of corrosion that had been initiated at the edges of the specimens.

The EIS specimens were cut to appropriate sizes for mounting in epoxy. The samples were mounted in a manner that would expose only one of each of three orthogonal planes that were parallel and/or perpendicular to the rolling direction of the sheet. Henceforth, these exposed planes will be called the rolled surface, the long transverse edge (perpendicular to the rolled surface and containing the rolling direction) and the short transverse edge (perpendicular to both the rolled surface and the rolling direction), respectively. Prior to mounting, provisions were made for electrical connection to the unexposed back of the samples and the unexposed edges were coated with an aluminum-vinyl anticorrosive paint to prevent crevice corrosion between the epoxy mount and the aluminum electrodes. After mounting, the specimens were polished (using 240, 400 and finally 600 grit papers) and cleaned with dichloromethane and acetone.

For each experiment, a pair of identical aluminum specimens (same alloy and same exposed face) were immersed in a 2 ℓ beaker containing a solution of 3% sodium chloride for 14 days. Each cell was equipped with an air purge and a saturated calomel reference electrode brought into close proximity with one electrode by a Luggin probe. The mounted specimens were separated by 2.5 mm and kept in a stable parallel position with plastic holders.

Electrochemical impedance measurements were performed with a commercial generator/analyzer (Solartron Model 1255) at the corrosion potential and always taken in the direction of decreasing frequency. A potentiostat was not used in these measurements. The alternating current was applied between the two aluminum electrodes and kept at a value which would not cause more than 10 mV difference (peak to peak) across the cell. The reference electrode served only to measure electrochemical potential noise, which was independently monitored between EIS measurements. A custom-made multiplexer directed the inputs from each technique. The measurements could be performed automatically for up to eight cells in any order and in time intervals specified by the user. Polarization resistance values (R_p) were determined automatically during

P150275.PDF [Page: 5 of 14]

experiments and the data were analyzed for their deviations from the semi-circle of a Nyquist representation.

At the completion of these experiments, the specimens were removed and examined with both optical and scanning electron microscopy to observe any differences in corrosion morphologies.

Finally, two new sets of 2090 panels were subjected to full immersion in sea water for three months. One set was prepared with sheared edges like those used in the earlier long term exposure tests while the edges of the other set were polished using progressively finer grit papers ranging from 80 to 600 grit. This procedure resulted in the removal of approximately 0.4 mm of material from each edge and produced a surface similar to that used in the EIS experiments.

RESULTS AND DISCUSSION

Long Term Exposures

A summary of the results of the long term exposures is shown in Table 2. After the exposure to the sea water fog, crevice corrosion had initiated under one site on the 8090 alloy. Some minor corrosion was also observed along rolling marks that became visible after the exposure. Deep pits were observed on the surface of the 2024 alloy, which also suffered crevice corrosion under six of the twenty-four initiation sites , with three of these sites showing substantial penetration. Deep pits were also observed on the surface of the 2090 alloy but crevice corrosion had not been initiated. Pitting had occurred on the surface of the 7075 alloy as well, but the depth of attack was not as severe as that which occurred on either the 2090 or 2024 alloy. This observation was consistent with the higher copper concentration present in the 2000-series alloys. Crevice corrosion was observed under one initiation site on the 7075 alloy.

In all cases, the specimens that were completely immersed in sea water showed a reduction in the intensity (depth of penetration) of corrosion, if any, in the crevices from that observed in the sea water fog exposures. This suggests that the corrosion that occurred in the crevices in the fog exposures was more a result of moisture retention in the crevices than a result of mechanisms such as differential aeration that are normally associated with crevice corrosion. The rolled surface of the 8090 sheet showed selective corrosion, without deep pits, that etched the surface in a manner which served to highlight the rolling direction of the sheet without causing much metal loss. Corrosion of the surface of the 2024 alloy was characterized by a large number of deep pits. Corrosion of the 2090 alloy occurred in the form of a smaller number of broad pits that were scattered over the surface. The number and severity of these pits increased near the edges of the panel. The surface of the 7075 alloy was characterized by a larger number of pits than the 2090, with the average pit on the 7075 having a smaller surface area.

The partial immersion test presented the toughest challenge to the alloys because the air/water interface created the possibility of differential aeration cells resulting from changing oxygen concentrations as a function of distance from the interface. In all cases, the interface was near the central hole. The rolled surface of the 8090 sheet suffered the least corrosion under these circumstances. In addition to the corrosion of the immersed surface described previously, several isolated but deep pits were observed at the air/water interface, as shown in Figure 1. Corrosion of the wetted area of the 2024 sheet was as severe as previously described but no additional corrosion was attributed to the presence of the air/water interface (Figure 2). The 2090 alloy surface appeared as before, with the addition of extensive corrosion at and just above the air/water interface (Figure 3). In this case the corrosion products produced at the interface crept up the panel, bringing along sea water by capillary action. The resulting "poultice" produced an excellent environment for the corrosion that ensued. A similar phenomenon was observed on the 7075 sheet (Figure 4).

The extent and type of corrosion on the edges of the exposed panels were often quite different than those found on the rolled surfaces. The 8090 panel exhibited one large pit on one of the edges but was essentially unattacked elsewhere. The edges of the 2024 panel exhibited two pits, one of which had initiated on the edge while the other was associated with a pit on the rolled surface. Large cracks were observed on the edges of the 7075 panel. These cracks are consistent with the development of intergranular cracking, to which 7075 is known to be susceptible. The edges of the 2090 and 6061 panels were essentially unaffected by the fog exposure.

The 8090 panel that was completely immersed in sea water exhibited only superficial corrosion on the rolled surfaces, while being severely attacked on the edges in a manner consistent with the selective corrosion often associated with intergranular cracking. This observation was confirmed by metallographic examination, which showed extensive intergranular cracking associated with the corrosion that had been initiated on the edge. The 2024 panel was severely corroded along the edges, with a combination of pitting of the edge and selective attack. No evidence of intergranular cracks associated with this corrosion could be found.

The 6061 panel showed some pitting along both edges. Although 6061 is known to be susceptible to shallow pitting in sea water, the observed intensity of attack was somewhat surprising. This was attributed to copper ions which plated out of the sea water after being introduced into it from the corroding 2000-series alloys in the partial immersion test that was conducted 1 m upstream. This hypothesis is supported by the lack of pitting observed on the 6061 panel in the partial immersion test. In this case the copper ions released from the 2000-series alloys were carried

P150275.PDF [Page: 6 of 14]

downstream before they could affect the 6061 panel.

Metal loss on the edges of the 2090 panel was primarily associated with pits that occurred on the rolled surfaces. Several pits that appeared to have been formed in the centre of an edge were actually found to be part of a larger pit that had initiated on the rolled surface and then undercut the surface until they became visible again at an edge. One "crack" was found which did appear to have been initiated at the edge of the specimen. Metallographic examination revealed intergranular cracks at the base of the pit that resulted from the corrosion at this site. The 7075 panel showed virtually no corrosion along one edge and severe selective attack along each of the other three edges. The lack of corrosion of the one edge was considered to be anomalous as 7075 is known to be susceptible to corrosion in sea water[18]. This conclusion was supported by the observation of corrosion on all four edges of the salt fog specimens, which were exposed to a less aggressive environment than full immersion. Evidence of extensive intergranular cracking was also found on this specimen.

Figure 5 shows one of the edges of the panels that were partially immersed in sea water. The edge shown in this photograph was completely immersed in the sea water and, except for the observation that the 7075 panel showed selective attack along both immersed edges and the absence of corrosion on the 6061 panel as discussed previously, appeared similar to those of the specimens that had been completely immersed. One of the edges of the 7075 panel showing selective attack was the corresponding edge to the one which did not corrode in the full immersion exposure, adding support to our treatment of the edge that did not corrode as anomalous.

The effects of shearing or polishing the edges of the AA 2090-T8 panels after immersion in sea water for 4 months are shown in Figure 6. These effects are discussed in more detail in the section on the results of EIS.

Electrochemical Impedance Spectroscopy

The average corrosion rates, determined from the polarization resistance measurements, and the average depression angles for each face of each alloy are shown in Table 3. According to the polarization resistance data, the 8090 alloy showed roughly equal corrosion rates for all three faces. With the assumption that the angle of depression increases with increased pitting, the EIS data indicated that the rolled surface of the 8090 had the lowest pitting rate, followed by the long transverse edge and the short transverse edge, which had the highest rate. Examination of the surfaces of the EIS specimens with optical and scanning electron microscopy suggested that the correlation between angle of depression and pitting rate involved the number of pits formed in any given area (pit density) rather than the pit depth (Figure 7). The low pitting rate suggested by EIS for the rolled surface was consistent with visual observation of the long term exposure panels. However, the approximate equivalence of the corrosion rates for all three faces was not. If the interpretation of the EIS data is correct, the corrosion of the rolled surface must occur at this high rate during the initial 14 days in which EIS data was collected, but then fall to a very low value over the longer term. The polarization resistance data for the 2024-T3 alloy showed a pronounced difference in overall corrosion rate between its rolled surface and its edges, with the edges having consistently higher rates. A similar trend was observed for the angle of depression, the average of which would fall to about 13° without the data points collected in the first 50 hours. These results are consistent with observations made on the long term exposure panels, which were characterized by a higher density of localized corrosion sites on the edges.

On the basis of the EIS data, the conclusion would be reached that the edges of the 8090-T851 alloy had lower overall corrosion rates and were less prone to pitting than their 2024-T3 counterparts. The edges of the 8090 long term exposure panels had substantial areas where no visible corrosion occurred. This could be consistent with the lower overall corrosion rates and lower pitting density suggested by EIS in comparison with 2024. However, the depth of attack within each pit was as large or larger than a corresponding pit on 2024. Thus the rate of corrosion within a pit was as least as severe for 8090 as for 2024. EIS alone gave no indication of this phenomenon, which was also observed on the EIS specimens when they were examined after they were removed from the electrochemical cell. The polarization resistance values for the rolled surfaces of the 8090 and 2024 were approximately equal. This result does not correlate with the appearance of the long term exposure panels. As discussed previously, corrosion of the rolled surface of the 8090 must initially occur at a high rate, but then fall to a much lower value over the longer term. The lower pitting density suggested by EIS for the rolled surface of the 8090 was, however, consistent with visual comparison of the long term exposure panels.

According to the polarization resistance data, the rolled surface of the 2090-T8 specimens had a lower overall corrosion rate than either of the long transverse or short transverse edges, which were themselves corroding at roughly equal rates. The rolled surface also had a lower angle of depression than either of the edges throughout the duration of the experiment. As with the 8090 alloy, the angle of depression corresponds well with the number of pits found on these surfaces at the end of the experiment. This does not, however, correlate with the corrosion observed on the long term exposure panels. As previously discussed, most of the corrosion of the edges of these panels was associated with pits that had developed on the rolled surfaces. We postulated that this inconsistency between EIS and long term exposure experiments could be caused by the different methods of preparation of the edges. The exposed surfaces of the EIS specimens were cut and then polished whereas the original long term exposure

P150275.PDF [Page: 7 of 14]

panels had been sheared. The edges of these panels did not receive any subsequent preparation. The appearance of the edges of the two sets of 2090 specimens that were fully immersed in sea water for three months support this hypothesis. The polished edges showed pitting that had been initiated on the edges while most of the corrosion of the sheared edges was associated with pits that had developed on the rolled surfaces (Figure 6). Furthermore, the greatest depth of corrosion attack on the rolled surfaces of the panels with sheared edges occurred immediately adjacent to those edges. A similar phenomenon was not observed on the specimens with polished edges. Thus the cold work associated with shearing appeared to reduce the initiation of corrosion on the edges. This conclusion was supported by the corrosion observed around the identifying numbers that had been scratched into the rolled surfaces. The numbers themselves suffered no corrosion while the surrounding surfaces had been preferentially corroded to the extent that the depressions created by the scratches became higher than the adjacent material. Slife[6] also postulated that cold work could have an effect on the corrosion rate of AA 2090.

The corrosion rate determined by polarization resistance for the rolled surface of the 7075 was higher than that measured for the edges. This was not consistent with the appearance of the long term panels, which suffered more metal loss along the edges than the rolled surface. The angle of depression data indicated that the rolled surface of the 7075 had the lowest pitting density, while the long transverse and short transverse edges had higher rates. These results did correlate very well with the long term exposure tests, in which the edges did indeed suffer much worse localized attack.

According to the polarization resistance data, the rolled surface of the 2090 alloy had a consistently lower corrosion rate than the same surface of the 7075. This did not appear to be consistent with the long term exposure tests, in which corrosion damage seemed to be more extensive on the surface of the 2090 alloy. On the other hand, the polarization resistance data suggested that the edges of the 2090 were only slightly more corrosion resistant than the 7075 edges. Once again, this did not appear to be consistent with visual observation of the long term exposure panels. In this case, the edges of the 2090 panels, whether sheared or polished, suffered noticeably less corrosion than their 7075 counterparts. The angle of depression data indicated that the pit density should be lower on the rolled surface of the 2090 than the 7075 and that the pit density should be much lower on the edges of the 2090 than the 7075. These results are completely consistent with the appearance of the long term exposure panels. As was the case for the comparison between the 8090 and 2024 alloys, the angle of depression data for the 2090 and 7075 alloys provided a better correlation with the long term exposure tests than the polarization resistance measurements. However, as in the case of the 8090 alloy, the correlation involved only the pit density, not the rate of attack within each pit (Figure 8).

CONCLUSIONS

The long term exposure tests indicated that the rolled surfaces of the 8090-T851 sheet were more resistant to corrosion than the conventional 2024-T3 sheet. Except for some pits which developed at an air/water interface, these surfaces suffered only minor corrosion which highlighted rolling marks in the 8090 sheet. Although this material did suffer corrosion under one crevice in the exposure to sea water fog, the attack was less severe than that observed on the 2024. However, the 8090 experienced severe localized attack along edges that were immersed in sea water. A smaller proportion of the surface area of the 8090 edges was attacked than of the 2024, but the depth of attack within a corroding area was at least as severe as for 2024.

The corrosion rate determined by polarization resistance for the rolled surface of 8090 appeared to be much higher, in relation to the edges and to the rolled surface of the 2024, than that observed on the long term exposure panels. Examination of the EIS specimens with optical and scanning electron microscopy suggested that a correlation existed between the angle of depression and the number of pits in a given area. Conclusions drawn from the angle of depression data were consistent with the appearance of the long term specimens.

Evidence of intergranular corrosion was not found on the 2024 specimens. Severe intergranular cracking was found to be associated with the pitting initiated at the edges of the 8090 alloy. Unless care is taken to seal the edges of components made from 8090-T851 and to deny access of sea water to crevices, then corrosion failures can be expected to occur even though exposed surfaces of the alloy may appear undamaged.

The long term exposure tests indicated that the rolled surfaces of the 2090-T8 sheet suffered as much or more corrosion damage than their counterparts on the 7075-T6 sheet. Some fairly deep pits occurred on the rolled surfaces of the 2090, even in the exposure to sea water fog. This result was not surprising, given the higher copper concentration in the 2090 alloy. However, increased corrosion was not observed under the crevice initiation sites and localized corrosion was substantially reduced along the edges. Both alloys showed extensive corrosion under a poultice of corrosion products at the air/water interface in the partial immersion test. Intergranular cracking was observed at the base of a pit on the edge of a 2090 panel, while extensive intergranular cracking was found on the 7075 panels. Such cracking can, of course lead to structural weakness without much visible corrosion. Thus, the 2090 alloy does appear to offer some advantages over 7075-T6 sheet. Corrosion initiated at edges, whether pitting or intergranular cracking, is very difficult to detect on an aircraft structure. The 2090 sheet appears to be more resistant to corrosion at the edges than the 7075. Corrosion

P150275.PDF [Page: 8 of 14]

of the rolled surfaces of the 2090 sheet can easily be controlled by the proper application of protective coatings.

The angle of depression data was found to correlate well with the pit density observed on the rolled surface and edges of the 2090 EIS specimens, but not with the long term exposure panels. Additional tests suggested that the corrosion resistance of the edges of the long term panels was due, in part, to cold work associated with shearing. Nonetheless, even the edges of cut and polished specimens of 2090 showed much less corrosion than their 7075 counterparts. As was the case for the 8090 alloy, the polarization resistance data suggested a higher corrosion rate for the rolled surface of the 7075 than that observed in the long term exposure tests. However, the angle of depression data correlated very well with the appearance of the long term panels. Furthermore, conclusions drawn from the angle of depression data on the comparative behaviour of the 2090 and 7075 alloys were completely consistent with those drawn from the appearance of the long term panels.

Because the polarization resistance measurements resulted in corrosion rates for the rolled surfaces of 8090 and 7075 that were too high in relation to their edges and to the alloys against which they were compared, the angle of depression of the Nyquist plots provided a better correlation with visual observations of the long term exposure panels. However, the EIS measurements were apparently insensitive to the existence of intergranular cracking and to the rate of corrosion within a pit. Thus, EIS can be a useful technique for rapidly assessing the relative corrosion resistance of different aluminum alloys but cannot be used in isolation to completely characterize the corrosion resistance of an alloy.

REFERENCES

1. W. E. Quist and G. H. Narayanan, "Aluminum-Lithium Alloys" in "Treatise on Materials Science and Technology", edited by A. K. Vasudevan and R. D. Doherty, Vol. 31, pp. 219-250 (1989)
2. R. J. H. Wanhill, L. Schra and W. G. J. Hart, International Conference AIM/ASM on Evolution of Advanced Materials, Milano, Italy, 31 May-2 June 1989
3. S. J. Ketcham and J. J. de Luccia in "Aircraft Corrosion", AGARD Conf. Proc. No. 315 (1981)
4. C. J. E. Smith, J. A. Gray, L. Schra and J. A. M. Boogers in "New Light Alloys", AGARD Conf. Proc. No. 444
5. R. G. Buchheit Jr., J. P. Moran and G. E. Stoner, Corrosion, Vol. 46, pp. 610-617 (1990)
6. R. I. Slife, Corrosion 88 Conf., St. Louis, Paper No. 385, NACE
7. B. B. Bavarian and M. Zamanzadeh, Corrosion 88 Conf., St. Louis Paper No. 386, NACE
8. J. P. Moran, E. A. Starke Jr., G. E. Stoner and G. L. Cahen Jr., Corrosion, Vol. 43, pp. 374-382 (1987)
9. T. Sheppard and N. C. Parson, Mat. Science and Tech., Vol. 3, pp. 345-352 (1987)
10. R. T. Holt, Canadian Aeronautics and Space J., Vol 35, pp. 128-137 (1989)
11. K. Hladky, L.M. Callow and J.L. Dawson, Br. Corros. J., Vol. 15, pp 20-25 (1980)
12. M.W. Kendig, E.M. Meyer and G. Lindberg, Corros. Sc., Vol. 23, pp. 1007-1015 (1983)
13. D.C. Silverman and J.E. Carrico, Corrosion, Vol. 45, pp. 280-287 (1988)
14. P.R. Roberge and R. Beaudoin, J. Appl. Electrochem., Vol. 18, pp. 38-42 (1988)
15. P.R. Roberge and R. Beaudoin, J. Appl. Electrochem., Vol. 18, pp. 601-607 (1988)
16. P.R. Roberge, E. Halliop, M. Asplund and S.V. Sastri, J. Appl. Electrochem., Vol 20, pp. 1004-1008 (1990)
17. P.R. Roberge, V.S. Sastri and V. Maxwell, Corrosion, Vol. 48, p. 333 (1992)
18. Godard, H.P., Jepson, W.B., Bothwell, M.R. and Kane, R.L., "The Corrosion of Light Metals", Wiley and Sons, New York, p. 140, (1967)

Table 1. Nominal composition of alloys tested, wt-%

Alloy	Li	Cu	Mg	Si	Fe	Mn	Zn	Zr
2024	-	3.8-4.9	1.2-1.8	0.5	0.5	0.3-0.9	0.25	-
2090	1.9-2.6	2.4-3.0	0.25	0.1	0.12	0.05	0.1	0.08-0.15
6061	-	0.15-0.40	0.8-1.2	0.4-0.8	0.7	0.15	0.25	-
7075	-	1.2-2.0	2.1-2.9	0.4	0.5	0.3	5.1-6.1	-
8090[a]	2.35	1.23	0.67	0.02	0.03	0.001	0.02	0.11

Note a: Actual heat analysis for the material supplied by ALCAN

P150275.PDF [Page: 9 of 14]

Table 2. Results of long term exposure tests.

Alloy	Salt Fog		Total Immersion		Partial Immersion (air/water interf.)
	rolled surface	minor	rolled surface	minor selective corr.	a few deep pits
8090-T851	edges	1 pit	edges	severe selective attack (cracking)	
	crevices	1 site			
	rolled surface	many deep pits	rolled surface	many deep pits	no additional corrosion
2024-T3	edges	2 pits	edges	severe pitting and selective attack	
	crevices	6 sites			
	rolled surface	deep pits	rolled surface	broad pits	extensive "poultice" corrosion
2090-T8	edges	no attack	edges	pits initiated on rolled surface	
	crevices	none			
	rolled surface	shallow pits	rolled surface	many small pits	extensive "poultice" corrosion
7075-T6	edges	large cracks	edges	severe selective attack	
	crevices	1 site			

Table 3. Average corrosion rates from polarization resistance measurements and average depression angles during 14 days of exposure.

Alloy	Face	Corrosion Rate (mm/y)	Angle of Depression (degrees)
8090-T851	Rolled Surface Long Transverse Short Transverse	0.05 0.04 0.03	6 12 17
2024-T3	Rolled Surface Long Transverse Short Transverse	0.05 0.16 0.22	17 21 23
2090-T8	Rolled Surface Long Transverse Short Transverse	0.06 0.08 0.09	10 16 19
7075-T6	Rolled Surface Long Transverse Short Transverse	0.14 0.11 0.12	12 33 29

P150275.PDF [Page: 10 of 14]

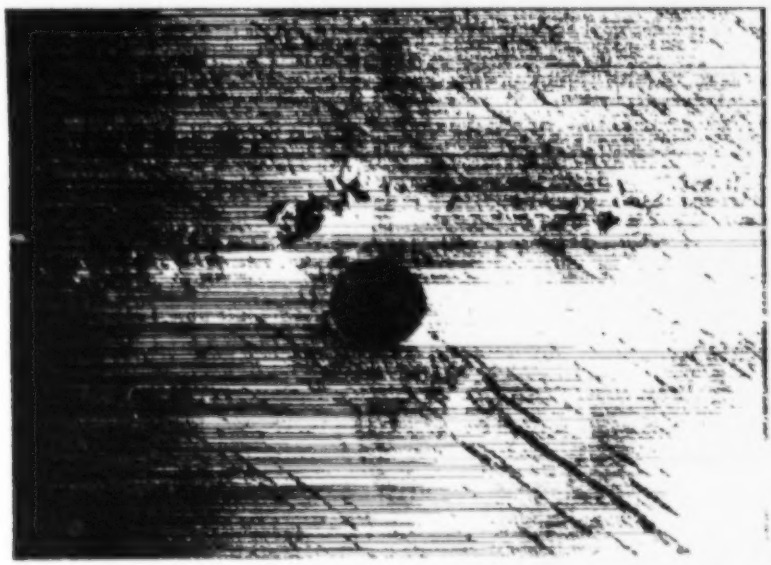

Figure 1. Appearance of AA 8090-T851 panel after partial immersion in sea water for four months. The air/water interface was near the top of the central hole.

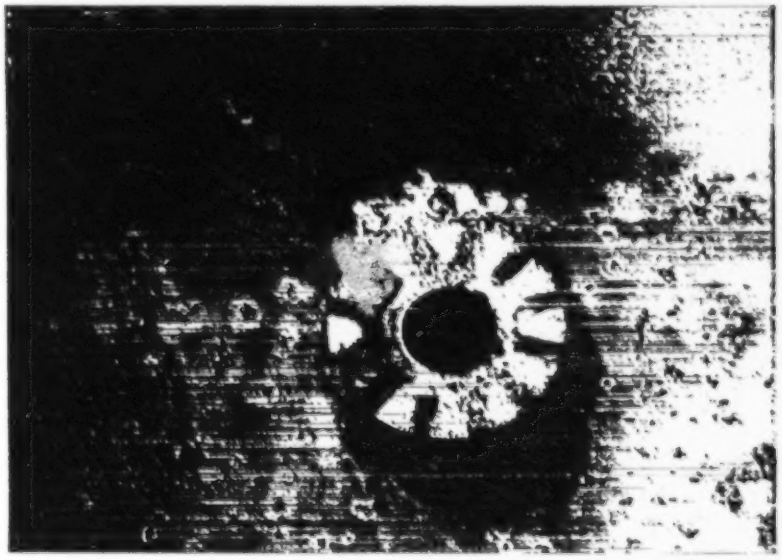

Figure 2. Appearance of AA 2024-T3 panel after partial immersion in sea water for four months. The air/water interface was near the top of the central hole.

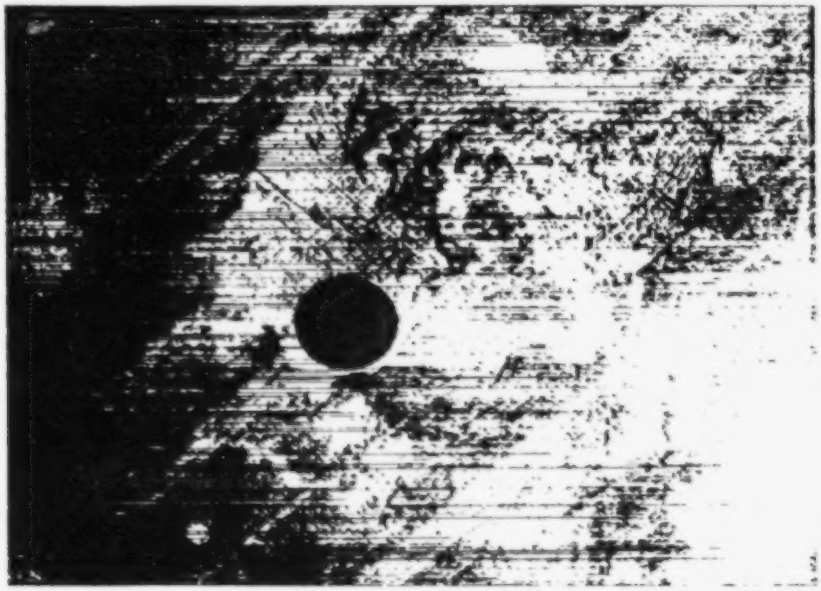

Figure 3. Appearance of AA 2090-T8 panel after partial immersion in sea water for four months. The air/water interface was near the top of the central hole.

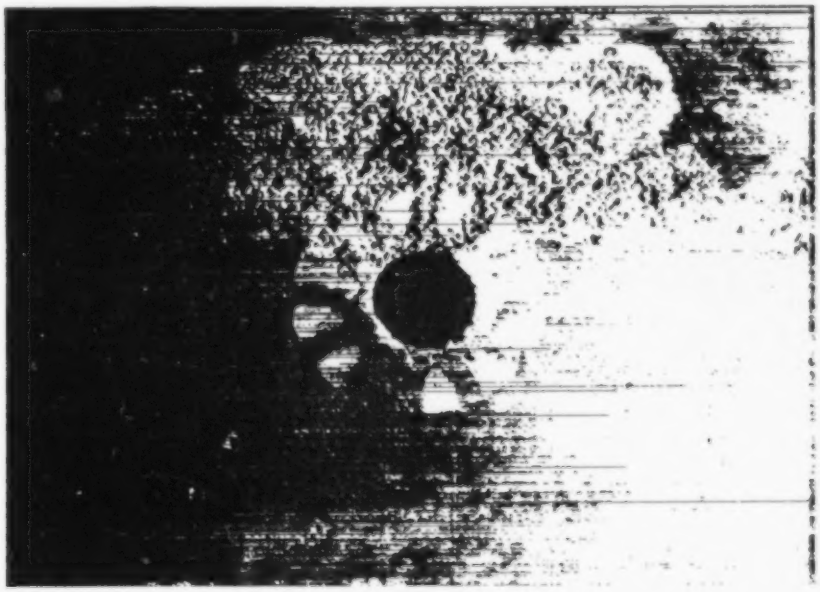

Figure 4. Appearance of AA 7075-T6 panel after partial immersion in sea water for four months. The air/water interface was near the top of the central hole.

P150275.PDF [Page: 12 of 14]

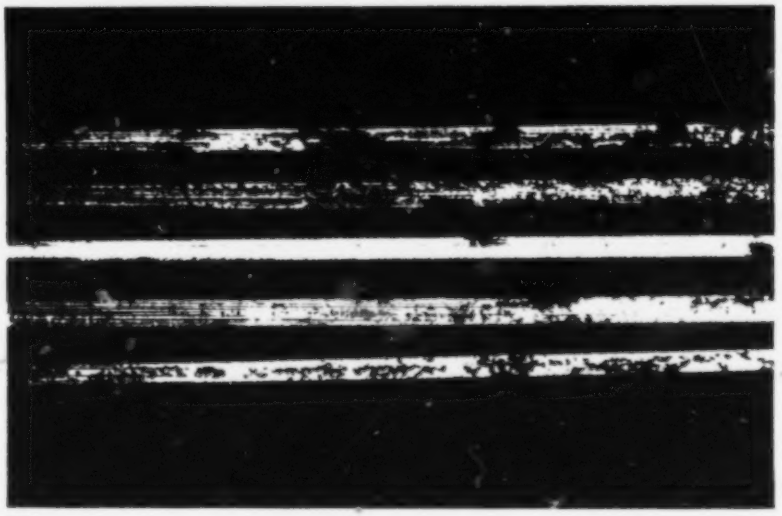

Figure 5. Appearance of the edges of the aluminum panels partially immersed in sea water for four months. These edges were completely immersed throughout the test. From top to bottom: (i) 8090-T851, (ii) 7075-T6, (iii) 6061-T6, (iv) 2090-T8 and (v) 2024-T3.

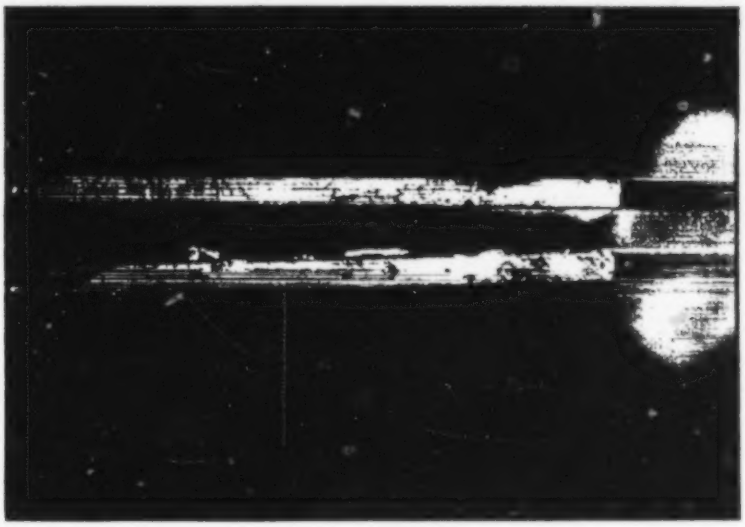

Figure 6. Appearance of the edges of the AA 2090-T8 panels after immersion in sea water for four months. The top panel has sheared edges while the edges of the lower panel were polished.

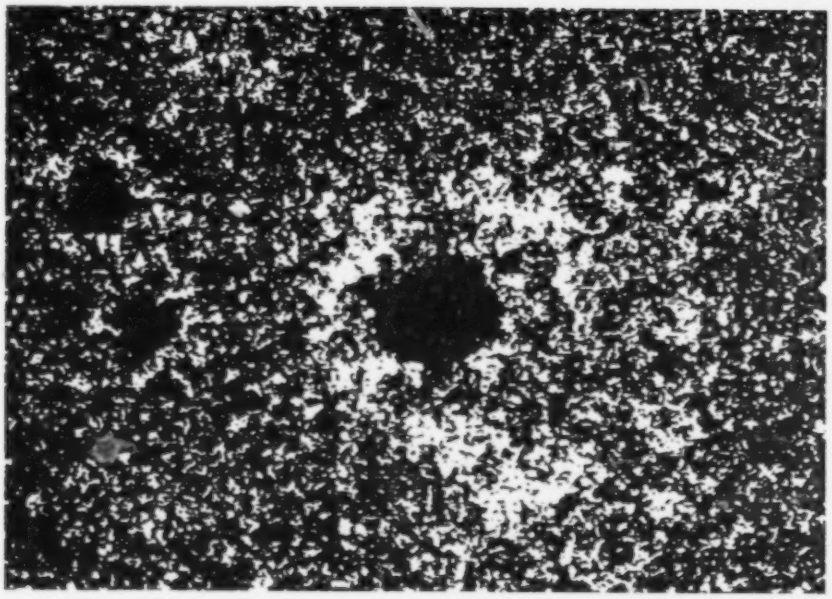

(a)

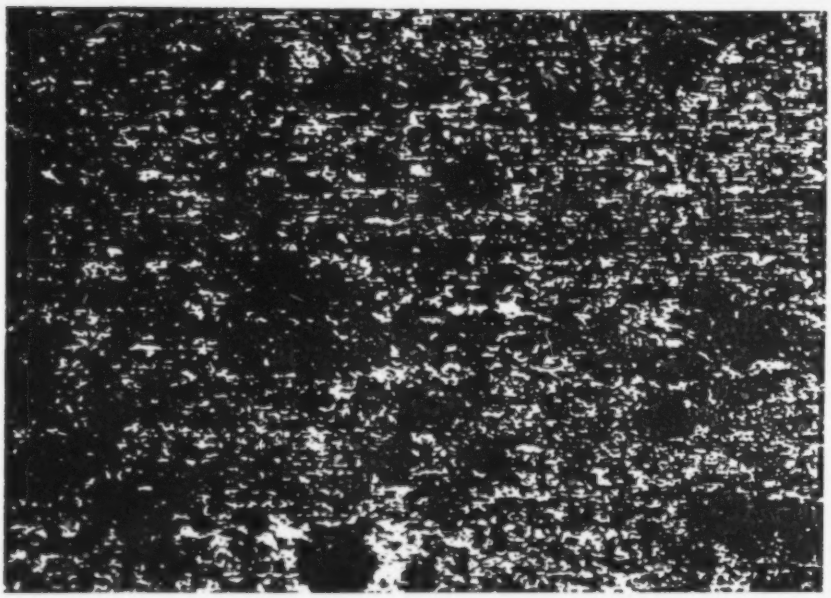

(b)

Figure 7. Micrographs of two surfaces of AA 8090-T851 at the end of the EIS experiments. (a) Rolled surface. (b) Long transverse edge. 100x.

P150275.PDF [Page: 14 of 14]

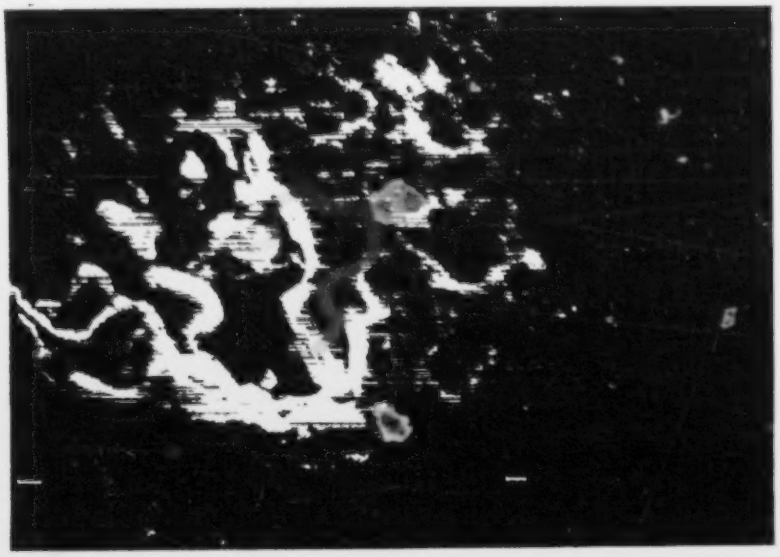

(a)

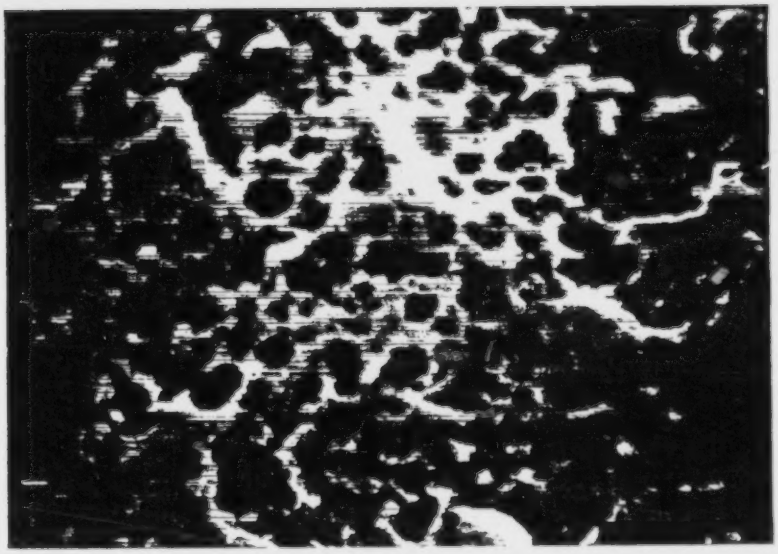

(b)

Figure 8. Scanning electron micrographs of short transverse edges after EIS experiments for: (a) 2090-T8 (b) 7075-T6. 700x.